IOP PUBLISHING JOURNAL OF PHYSICS D: APPLIED PHYSICS

J. Phys. D: Appl. Phys. **41** (2008) 025206 (7pp) doi:10.1088/0022-3727/41/2/025206

# On the existence of transiently negative diffusion coefficients for electrons in gases in $E \times B$ fields

**R D White[1], S Dujko[1], K F Ness[1], R E Robson[2], Z Raspopović[3] and Z Lj Petrović[3]**

[1] ARC Centre for Antimatter–Matter Studies, School of Mathematics, Physics and Information Technology, James Cook University, Townsville 4810, Australia
[2] ARC Centre for Antimatter–Matter Studies, Research School of Physical Sciences, Australian National University, Canberra 2600, Australia
[3] Institute of Physics, University of Belgrade, PO Box 68, 11080 Zemun, Belgrade, Serbia and Montenegro

E-mail: Ronald.White@jcu.edu.au

Received 26 October 2007, in final form 14 November 2007
Published 4 January 2008
Online at stacks.iop.org/JPhysD/41/025206

**Abstract**
A recent study (Raspopović Z *et al* 2000 *J. Phys. D: Appl. Phys.* **33** 1298) reported the existence of negative diagonal diffusion tensor elements for electrons in a neutral gas under the influence of crossed radiofrequency electric and magnetic fields. In this paper we demonstrate, using a time-dependent multi-term solution of the Boltzmann equation and time-resolved Monte Carlo simulation, that this phenomenon is a transient relaxation effect obtainable under dc crossed field conditions.

(Some figures in this article are in colour only in the electronic version)

## 1. Introduction

Recently there has been considerable research aimed at the prediction of electron transport in gases under the influence of RF electric (see e.g. the reviews [2–5]) and RF electric and magnetic fields (see e.g. [1–3]) motivated by the vast applications of capacitively and inductively coupled plasmas [6, 7]. These studies have unearthed a wide variety of anomalous kinetic phenomena, i.e. phenomena that cannot be directly extrapolated either from steady-state dc results or from individual particle trajectories. Importantly they indicate that more detailed models of transport in capacitively and inductively coupled plasmas may be required in order to account for such effects. These studies, although in the 'swarm' limit, provide a benchmark for plasma models in the limit of low electron density [8].

This investigation was motivated by studies of the anomalous behaviour of the longitudinal diffusion coefficient $D_E$[4] (diffusion along the electric field direction) under the action of RF electric fields [9–12]. Recently, Petrović and co-workers at Belgrade University extended their Monte Carlo simulations techniques to include the combined action of RF electric and magnetic fields [1]. The study unearthed a striking new phenomenon—the existence of a negative diffusion coefficient along the $E \times B$-direction at certain phases of the field. These results were independently validated using a Boltzmann equation solution [3] and it was shown that the transient negative behaviour could also appear for diffusion in the $E$-direction. Although the initial results were for a standard benchmark model interaction cross-section, these results were subsequently shown to be present in a number of real gases [2, 13].

The anomalous behaviour in $D_E$ in RF electric fields [10, 11] can be best understood by a study of transient behaviour under the action of step function electric fields [14]. In this study, we aim to extend this approach to come to terms with the anomalous behaviour of transport coefficients in RF electric and magnetic fields [1, 3]. Transient studies have previously been performed in both pure dc electric fields (see, e.g. [4, 5, 15–17]), RF electric fields (see, e.g. [5, 18, 19]) and

[4] In this paper we label the axes along the perpendicular directions of the electric field $\boldsymbol{E}$, magnetic field $\boldsymbol{B}$ and along the $\boldsymbol{E} \times \boldsymbol{B}$ vector.

 

in dc electric and magnetic fields [2, 13, 20]. Of particular note for this paper is the *two-term* Boltzmann equation study of Loffhagen and Winkler [20], who considered the explicit effect of a magnetic field on the relaxation of electron swarms in atomic gases, focusing on spatially homogeneous (or spatially averaged) transport properties only (e.g. drift velocity or mean energy). This study represents an extension of their earlier work [20] by (i) considering transport properties of spatially inhomogeneous electron swarms (in particular diffusion tensor coefficients) and (ii) using a *multi-term* solution of Boltzmann's equation capable of handling velocity distributions with strong anisotropy. The results are validated using a time-resolved Monte Carlo simulation technique [2]. This paper focuses on the influence of an orthogonal magnetic field on the *transient* behaviour of the diagonal diffusion tensor elements. The relaxation of these coefficients is equally important for a basic understanding of temporal transients and their application in corrected plasma theories such as the relaxation continuum model [7, 21], although we do not make any detailed comparison here.

In section 2 we present a brief description of techniques used for the time-dependent multi-term solution of Boltzmann's equation and time-resolved Monte Carlo simulation for inhomogeneous electron swarms under the influence of electric and magnetic fields. In section 3 we highlight some important transient behaviour of the diagonal elements of the diffusion tensor and give a physical explanation of the phenomena present. The results of other transport properties including the drift velocity and mean energy are presented in appendix A.

## 2. Theory

### *2.1. Time-dependent multi-term solution of Boltzmann's equation*

The behaviour of electrons in gases under the influence of electric and magnetic fields is described by the phase-space distribution function $f(\boldsymbol{r}, \boldsymbol{c}, t)$ representing the solution of the Boltzmann equation

$$\frac{\partial f}{\partial t} + \boldsymbol{c} \cdot \frac{\partial f}{\partial \boldsymbol{r}} + \frac{q}{m}[\boldsymbol{E} + \boldsymbol{c} \times \boldsymbol{B}] \cdot \frac{\partial f}{\partial \boldsymbol{c}} = -J(f, f_0), \qquad (1)$$

where $\boldsymbol{r}$ and $\boldsymbol{c}$ denote the position and velocity co-ordinates, $q$ and $m$ are the charge and mass of the swarm particle and $t$ is time. The electric and magnetic fields are assumed spatially homogeneous and orthogonal with magnitudes $E$ and $B$, respectively. Swarm conditions are assumed to apply and $J(f, f_0)$ denotes the rate of change of $f$ due to binary particle-conserving collisions with the neutral molecules only. The neutral molecules are assumed to remain in thermal equilibrium, characterized by a spatially homogeneous phase-space distribution function $f_0(\boldsymbol{c}_0)$. In other words, swarm conditions are the unperturbed limit of ionized gases, perturbed neither by the space-charge fields nor by the effect of increased populations of excited states produced by inelastic and non-conservative collisions. The original Boltzmann collision operator [22] and its semiclassical generalization [23] are used for elastic and inelastic processes, respectively. We employ a co-ordinate system in which $-\boldsymbol{E}$ defines the $z$-axis, while $\boldsymbol{B}$ is in the $y$-direction.

Solution is made through the following representations of the phase-space distribution function $f$:

(i) Resolution of the angular dependence in velocity space: the angular dependence is represented in terms of a spherical harmonic expansion

$$f(\boldsymbol{r}, \boldsymbol{c}, t) = \sum_{l=0}^{\infty} \sum_{m=-l}^{l} f_m^{(l)}(\boldsymbol{r}, c, t) Y_m^{[l]}(\hat{\boldsymbol{c}}), \qquad (2)$$

where $Y_m^{[l]}(\hat{\boldsymbol{c}})$ are spherical harmonics and $\hat{\boldsymbol{c}}$ denotes the angles $(\theta, \phi)$ of $\boldsymbol{c}$. Note that it is imperative that for a full spherical harmonics expansion be considered in this situation. A simple Legendre polynomial representation (see e.g. [20]), with dependence on just one angle, is appropriate only for axially symmetric cases.

(ii) Projection of the space and implicit-time dependence of $f$: under hydrodynamic conditions the spatial dependence of the coefficients $f_m^{(l)}(\boldsymbol{r}, c, t)$ may be represented by an expansion in terms of powers of the gradient operator acting on $n(\boldsymbol{r}, t)$, the number density of electrons, namely, in spherical tensors, which takes the form

$$f_m^{(l)}(\boldsymbol{r}, c, t) = \sum_{s=0}^{\infty} \sum_{\lambda=0}^{\infty} \sum_{\mu=-\lambda}^{\lambda} f(lm|s\lambda\mu; c, t) G_\mu^{(s\lambda)} n(\boldsymbol{r}, t), \qquad (3)$$

where $G_\mu^{(s\lambda)}$ is the irreducible gradient tensor operator defined in [24].

(iii) Resolution of the speed dependence: the speed distribution functions are represented by an expansion about a Maxwellian speed distribution at a temperature $T_b$ in terms of modified Sonine polynomials:

$$f(lm|s\lambda\mu; c, t) = \omega(\alpha, c) \times \sum_{\nu=0}^{\infty} F(\nu lm|s\lambda\mu; \alpha, t) R_{\nu l}(\alpha c), \qquad (4)$$

where

$$w(\alpha, c) = \left(\frac{\alpha^2}{2\pi}\right)^{3/2} \exp\left\{\frac{-\alpha^2 c^2}{2}\right\}, \qquad (5)$$

$$\alpha^2 = \frac{m}{kT_b}, \qquad (6)$$

$$R_{\nu l}(\alpha c) = N_{\nu l} \left(\frac{\alpha c}{\sqrt{2}}\right)^l S_{l+1/2}^{(\nu)}\left(\frac{\alpha^2 c^2}{2}\right), \qquad (7)$$

$$N_{\nu l}^2 = \frac{2\pi^{3/2}\nu!}{\Gamma(\nu + l + 3/2)} \qquad (8)$$

and $S_{l+1/2}^{(\nu)}(\alpha^2 c^2/2)$ are Sonine polynomials and the $N_{\nu l}$ are defined such that the modified Sonine polynomials satisfy the orthonormality relation

$$\int_0^\infty w(\alpha, c) R_{\nu' l}(\alpha c) R_{\nu l}(\alpha c) c^2 \mathrm{d}c = \delta_{\nu'\nu}. \qquad (9)$$

The various properties of the moments due to symmetry and reality considerations are described in [25, 26].

The combined spherical harmonic and Sonine polynomial basis are the well known Burnett functions. The predominant advantage in the use of this basis set is the ability to consider the original Boltzmann collision operator [22] and its generalizations for inelastic and superelastic processes [23], without recourse to approximate forms in various limits [27].

Making use of the orthogonality properties of the basis functions, the following complex doubly infinite coupled differential equations are generated under conservative conditions [3]:

$$\sum_{\nu'=0}^{\infty}\sum_{l'=0}^{\infty}\sum_{m'=-l'}^{l'}\Bigg[\left(N\frac{\mathrm{d}}{\mathrm{d}t}\delta_{\nu\nu'}+n_0 J^{l}_{\nu\nu'}(\alpha)\right)\delta_{l'l}\delta_{m'm} + \mathrm{i}\frac{qE}{m}\alpha(l'm10|lm)\left\langle \nu l \parallel K^{[1]}(\alpha)\parallel \nu' l'\right\rangle\delta_{m'm} + \frac{1}{2}\frac{qB}{m}\Big\{\sqrt{(l-m)(l+m+1)}\,\delta_{m'm+1} - \sqrt{(l+m)(l-m+1)}\,\delta_{m'm-1}\Big\}\delta_{\nu'\nu}\delta_{l'l}\Bigg]F(\nu' l' m'|s\lambda\mu) = X(\nu lm|s\lambda\mu), \tag{10}$$

where

$$X(\nu lm|000)=0, \tag{11}$$

$$X(\nu lm|11\mu)=\sum_{\nu'=0}^{\infty}\sum_{l'=0}^{\infty}\Bigg[\left(-\frac{1}{\alpha}\right)(l'm-\mu 1\mu|lm) \times\left\langle \nu l \parallel \alpha c^{[1]}\parallel \nu' l'\right\rangle F(\nu' l' m-\mu|000)\Bigg] - \frac{(-1)^{\mu}}{\alpha}F(01-\mu|000)F(\nu lm|000). \tag{12}$$

Here $N$ is the neutral number density and $(l'm10|lm)$ is a Clebsch–Gordan coefficient [28]. The explicit expressions for the reduced matrix elements of the velocity ($\langle \nu l \parallel \alpha c^{[1]} \parallel \nu' l'\rangle$) and velocity derivative ($\langle \nu l \parallel K^{[1]}(\alpha) \parallel \nu' l'\rangle$) are given by [24]. Discretizing in time using an implicit finite difference scheme converts the system of coupled differential equations into a system of coupled matrix equations. We note that formally $\nu = 0, ..., \infty$, $l = 0, ..., \infty$ and $m = -l, ..., l$. Solution of (10) is made by truncation of the $\nu$ and $l$ indices to $\nu_{\max}$ and $l_{\max}$, respectively, and symmetry considerations imply that only non-negative $m$ are needed. These values are independently increased until the desired convergence criterion for the calculated transport properties of interest is obtained. $T_{\mathrm{b}}$ is a basis temperature parameter used to optimize convergence of the speed space expansion, i.e. to minimize the value of $\nu_{\max}$. From previous experience with steady-state calculations, a fixed $T_{\mathrm{b}}$ can give converged results only over a restricted range of applied fields (or equivalently mean energies). Hence, it is essential that this parameter is time-dependent to ensure convergence under time-dependent conditions. The block structure of the resulting equations is interesting, but has not been exploited at this stage.

The transport coefficient of interest are obtained from the following members of the hierarchy $(s, \lambda, \mu) = (0, 0, 0)$, (1,1,0), (1,1,1). In particular, the diagonal diffusion tensor elements of interest in this study can be expressed in terms of the calculated moments as follows:

$$\mathrm{ND}_{E\times B} = -\frac{1}{\alpha}\Big[\Re\{F(011|111)\}-\Re\{F(01-1|111)\}\Big], \tag{13}$$

$$\mathrm{ND}_{B} = -\frac{1}{\alpha}\Big[\Re\{F(011|111)\}+\Re\{F(01-1|111)\}\Big], \tag{14}$$

$$\mathrm{ND}_{E} = -\frac{1}{\alpha}F(010|110), \tag{15}$$

where $E$, $B$ and $E \times B$ refer to the directions (e.g. $D_B = D_{yy}$). $\Re\{\}$ refers to the real part of the moments. There are of course off-diagonal elements in the diffusion tensor but they are not considered in this paper.

This concludes our brief description of the theoretical formalism for the time-dependent multi-term solution of Boltzmann's equation for electron swarms under the influence of electric and magnetic fields. The reader is referred to the review [3] for complete details.

### *2.2. Brief discussion of the time-resolved Monte Carlo simulation*

We approach the Monte Carlo simulation of this problem in two stages. At time $t < 0$, electrons are initially released from the origin with a Maxwellian velocity distribution of 1 eV under the influence of electric field only. In order to optimize the simulation speed, the electron swarm has been scaled at fixed time intervals, by a factor of 2. This technique is based on simple duplication of somewhat relaxed electrons which are later followed independently [29]. The new born electron has the same co-ordinate and velocity as the original one. Therefore, we follow two identical electrons that describe the same trajectory. At the moment of the collision with the background particles these two identical electrons scatter into different directions and from that point their trajectories differ but their initial properties are closer to the relaxed swarm conditions. This technique does not change the energy distribution and allows an improvement in statistics of sampled properties. Some tests of this procedure over a wide range of conditions including the electric and magnetic field strengths, pressures and gas types have been made and results of testing indicate the validity and the numerical integrity of such an approach. After relaxation to the steady state in which both the swarm transport parameters and distribution function do not change in time, the multiplication of electrons is turned off. The magnetic field is applied at time $t = 0$ and the relaxation process is followed accurately in time. An extremely large number of electrons (typically $10^7$) have been followed in a neutral gas in order to retain the good statistics of the output data, particularly the diffusion coefficients. It is assumed that swarm conditions hold. All calculations are performed at zero gas temperature. In the present Monte Carlo code we follow the spatio-temporal evolution of each electron through time steps governed by the minimum of two relevant time constants: mean collision time and cyclotron period for the $\boldsymbol{E} \times \boldsymbol{B}$ field. These finite time steps are used to solve the integral equation for the collision probability in order to determine the time of the next collision. Once the moment of the next collision is established, the nature of the collision is determined by using

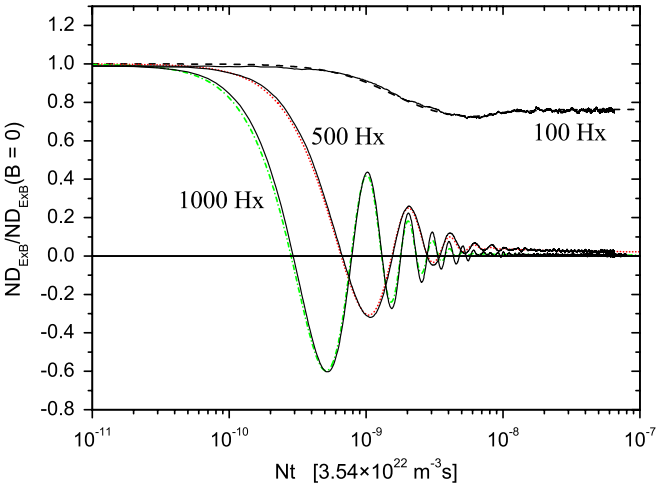


**Figure 1.** Temporal relaxation of the diagonal elements of the diffusion tensor for various applied magnetic fields for electrons in the Reid ramp model ($E/N = 12$ Td). The dashed lines represent the results from the time-dependent multi-term solution of Boltzmann's equation while the solid lines represent those from the Monte Carlo simulation.

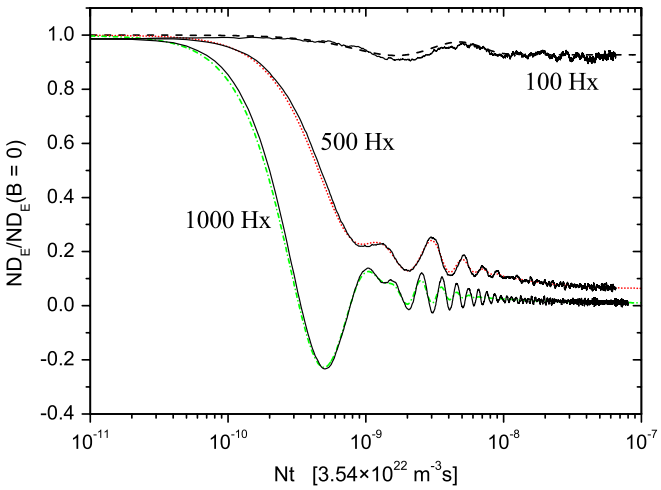


**Figure 2.** Temporal relaxation of $ND_E$ for various applied magnetic fields for electrons in the Reid ramp model ($E/N = 12$ Td). The dashed lines represent the results from the time-dependent multi-term solution of Boltzmann's equation while the solid lines represent those from the Monte Carlo simulation.

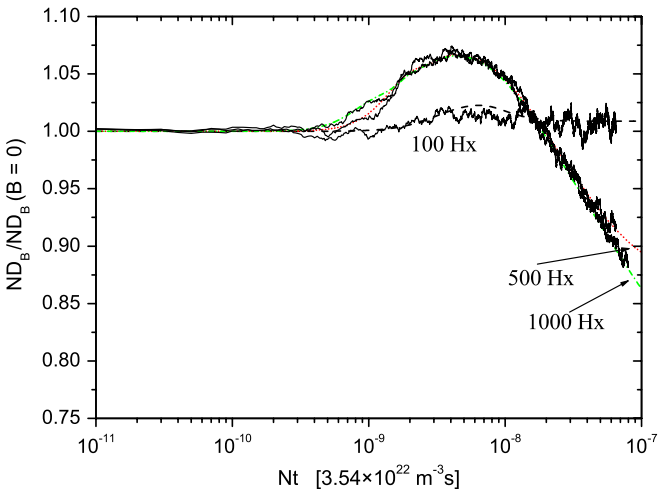


**Figure 3.** Temporal relaxation of $ND_B$ for various applied magnetic fields for electrons in the Reid ramp model ($E/N = 12$ Td). The dashed lines represent the results from the time-dependent multi-term solution of Boltzmann's equation while the solid lines represent those from the Monte Carlo simulation.

the relative probabilities of the various collision types. All electron scattering is isotropic for the model considered. It is important to note here that in the numerical relations for the electron trajectory in $\boldsymbol{E} \times \boldsymbol{B}$ fields, inaccuracies are introduced to trajectories due to the application of finite differences. That is often corrected by implementing a so-called Boris rotation in its original [30] and corrected form [1]. Here we use analytic solutions for the trajectories in between collisions. This is a somewhat slower procedure but the accuracy of trajectories is assured.

The definitions and corresponding formulae for the electron transport coefficients were given in our previous publications [2, 13]. Most importantly, sampling of various transport properties is always performed at times fully uncorrelated with the moments of collisions.

## 3. Results and discussion

In this investigation we follow [1] and use the Reid ramp model [31]. The primary aim of this work is to investigate the temporal response of the diffusive properties of the swarm to the application of an orthogonal magnetic field. The initial conditions represent the steady-state magnetic field free case where the electron swarm is acted on solely by a dc electric field ($E/N = 12$ Td, $B/N = 0$ Hx). At time $t = 0$, a crossed magnetic field is switched on (the electric field remains unaltered) and the relaxation properties of the swarm are monitored as a function of the normalized time, $Nt$. The steady state results are well documented [2, 19, 25, 32] and our results are in agreement with these earlier calculations. In this paper we focus entirely on the transient behaviour of the diffusion coefficients, and this behaviour is demonstrated in figures 1–3. In these figures we present and compare results from both a time-dependent multi-term Boltzmann equation solution and a time-resolved Monte Carlo simulation. The comparative agreement of results for all coefficients and all $B/N$ values considered supports the accuracy and integrity of both theories and associated codes.

As in the seminal work of Allis [33], we often find it convenient to refer to the charged-particle trajectories to explain certain phenomena. The following elementary considerations apply: in the absence of collisions, charged particles in electric and magnetic fields gyrate about the magnetic field lines at a frequency $\Omega = qB/m$ with a Larmour radius $r = mc_T/qB$, where $c_T$ is the tangential speed of the orbit. The guiding centres have a velocity $\boldsymbol{E} \times \boldsymbol{B}/B^2$. Superimposed on this picture is a component of the velocity in the $\boldsymbol{B}$-direction determined by the initial velocity of the charged particle in that direction. When collisions become important, the picture becomes more complicated. One must compare the gyration period ($\tau = \Omega^{-1}$) with the timescales for momentum ($\tau_m$) and energy ($\tau_e$) relaxation, although these vary according

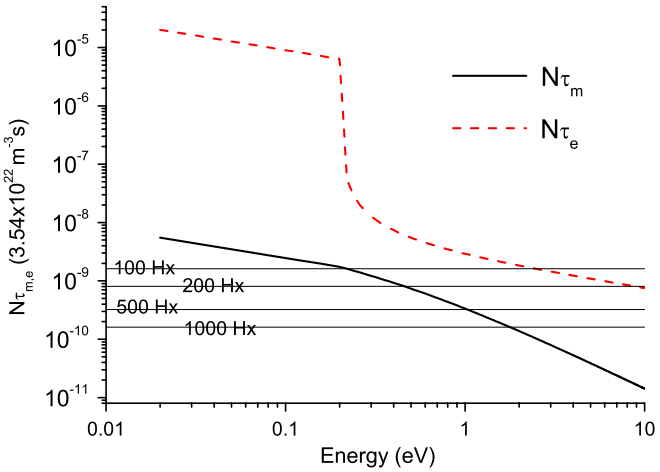


**Figure 4.** Comparison of the reduced cyclotron period for various $B/N$ (solid horizontal lines) with the reduced timescales for momentum and energy relaxation as a function of energy.

to the energy distribution of the swarm. The timescales are shown in figure 4. These three timescales are clearly evident in the relaxation profiles. During each relaxation profile however, the timescales $\tau_m$ and $\tau_e$ vary by virtue of the variation of the swarm's energy distribution. In general, the application of an orthogonal magnetic field decreases the mean energy of the swarm (see figure A2) and hence both $\tau_m$ and $\tau_e$ increase as a result. It then follows that we have a convolution of various processes and timescales for each, and this is demonstrated below.

In figure 1, we display the temporal relaxation of the $\boldsymbol{E} \times \boldsymbol{B}$ component of the diffusion tensor for a range of applied reduced magnetic fields. In general the profiles exhibit a damped oscillatory relaxation along a decaying profile for the $B/N$ considered. The period of the oscillation is governed by the gyro-period $\tau$ and the timescale for the envelope of the damped behaviour is determined by $\tau_m$. The timescale for the long term relaxation is governed by $\tau_e$. By virtue of the decrease in the mean energy as $B/N$ is increased, there is an associated increase in $\tau_e$ over each of the individual relaxation profiles. The oscillatory nature of the profiles is thus enhanced by increasing $B/N$ as the inequality $\tau < \tau_m$ is satisfied over a larger fraction of the profile. We also note that the time for $ND_{E\times B}$ to respond to the magnetic field (i.e. when the profiles depart from the initial conditions) appears to decrease monotonically with increasing $B/N$. Most importantly however, once the magnetic field reaches a certain threshold, the profiles of $ND_{E\times B}$ become *transiently negative*! For both the 500 Hx and 1000 Hx profiles, $ND_{E\times B}$ pass through zero and have a the peak negative excursion occurring at approximately at $\tau/2$.

In figure 2, we display the temporal relaxation of the longitudinal component of the diffusion tensor $ND_E$ for a range of $B/N$. We note that a similar behaviour with respect to the existence of oscillations exists for $ND_{E\times B}$. As $B/N$ is increased there is an increased oscillatory nature in the profiles. However, the amplitude of the oscillatory feature is not as pronounced as that of $ND_{E\times B}$. Most importantly we see that $ND_E$ also becomes transiently negative; however, the threshold of $B/N$ where this happens is greater than that for $ND_{E\times B}$. In addition, temporal relaxation for $ND_E$ is more complex during the first few periods of relaxation.

The temporal relaxation of $ND_B$ is displayed in figure 3. We note that unlike $ND_E$ and $ND_{E\times B}$, the profiles of $ND_B$ do not exhibit the damped oscillatory type relaxation nature. This is due to the fact that the Lorentz force does not act explicitly in this direction for the crossed field configuration. In addition the timescale for response to the application of the magnetic field is longer than that of $ND_E$ and $ND_{E\times B}$. Interestingly, however, and in contrast to $ND_{E\times B}$ and $ND_E$, we note for this model that the initial response of $ND_B$ to the application of an orthogonal field is to increase its value, leading to a transient peak structure dictated by the energy relaxation process and the nature of the cross-sections. In the long-time limit, i.e. the steady-state, an increase in $ND_B$ is observed for low fields such as 100 Hx. For this model, the time to the maximum in the peak structure appears to decrease for increasing $B/N$.

So physically, why does the phenomena of transient negative diffusion exist for the $\boldsymbol{E}$ and $\boldsymbol{E} \times \boldsymbol{B}$ components of the diffusion tensor? In general there are many physical factors that influence the diffusion when $\boldsymbol{E}$ and $\boldsymbol{B}$ fields are operative (see [26]). Fortunately, however, for the timescales involved, we can understand the phenomena of negative diffusion without extensive recourse to such arguments.

First let us consider diffusion in the $\boldsymbol{E} \times \boldsymbol{B}$-direction. If we consider the case of the highest $B/N$ shown, then when the magnetic field is switched on the condition $\tau < \tau_m$ is satisfied initially and the electrons on the average undergo gyrations about the $\boldsymbol{B}$ field before they undergo collisions. Since the initial velocity distribution has rotational symmetry about the $\boldsymbol{E}$-direction, the distribution of velocities in the positive and negative $\boldsymbol{E} \times \boldsymbol{B}$-directions are equal (figure A1 illustrates this point). If we consider pairing off all swarm particles which have $\boldsymbol{E} \times \boldsymbol{B}$ velocities that are equal in magnitude and opposite in sign, then it can be shown that the displacement in the $\boldsymbol{E} \times \boldsymbol{B}$-direction between these particles increases for the first quarter-period of gyration and then decreases for the next half-period, thus oscillating in time. Hence, the rate of change of displacement between these particles in the $\boldsymbol{E} \times \boldsymbol{B}$-direction also oscillates in time. That is, we have the situation where collectively the electrons on the average are approaching each other in the $\boldsymbol{E} \times \boldsymbol{B}$-direction and hence the swarm's diffusion coefficient in that direction becomes transiently negative. Of course for times greater than a few $\tau_m$, collisions begin to destroy this signature 'collisionless' behaviour and the decay of the oscillations then follows. For lower $B/N$ the collective 'collisionless' gyro-orbiting swarm behaviour cannot manifest itself since on average the electrons cannot complete orbits before undergoing collisions. Having said all this, we need to note that the effects of both fields are for most conditions only small perturbations on the otherwise chaotic particle trajectories. To support this we may note that the drift velocities are considerably smaller than the thermal velocities. Nevertheless, while the gyroscopic motion may be difficult to observe if one were to look at all trajectories, its imprint on the ensemble is distinguishable.

Now let us consider diffusion in the $\boldsymbol{E}$-direction. We can follow similar arguments to those used to describe diffusion

in the $\boldsymbol{E} \times \boldsymbol{B}$-direction though they must be modified by virtue of the initial condition. At $Nt = 0$, we have an anisotropic velocity distribution (i.e. the velocity distribution in the $\boldsymbol{E}$-direction differs from that in the perpendicular directions) which is displaced in the $-\boldsymbol{E}$-direction (figure A1 illustrates this point). There are more electrons travelling in the $-\boldsymbol{E}$-field direction than those traveling against it. If we follow similar arguments used for the $\boldsymbol{E} \times \boldsymbol{B}$-direction we can pair off some (but not all) electrons with velocities in the $-\boldsymbol{E}$-direction that are equal in magnitude but opposite in sign. We can monitor the displacement between each pair and again observe that this displacement oscillates in time. In contrast to the $\boldsymbol{E} \times \boldsymbol{B}$-direction, however, all electrons cannot be paired off in this case and the perturbations to the classical damped oscillatory profiles then follow. For the highest $B/N$ considered, the condition $\tau < \tau_{\mathrm{m}}$ is satisfied initially and this collisionless behaviour can manifest itself.

With this knowledge of the transient response of diffusion coefficients, we are now better placed to understand the profiles for RF crossed field conditions [1, 3]. It is well known that certain temporal behaviour for RF systems definitely cannot be understood in terms of the corresponding steady-state dc crossed field results [2, 3, 8] or from extrapolations of the dc results using the two distinct relaxation times for energy and momentum balance. To demonstrate this principle, in [14] the RF field was approximated by a series of dc step functions fields and the individual relaxations were monitored. In that study it was found that 'one must consider not only the ability of the transport property to relax on a time scale governed by the frequency of the field but also the implications associated with an inability to relax' [14]. Understanding of RF behaviour then reduces to understanding the transient behaviour and this was partial motivation for this paper. The application to the phenomena in [1, 3] will be addressed in future work.

## 4. Concluding remarks

In this paper we have investigated the temporal variation of the diagonal diffusion coefficients in response to the application of an orthogonal magnetic field. We have used two independent techniques, a time-dependent multi-term solution of Boltzmann's equation and a time-resolved Monte Carlo simulation. The agreement of the results of the two techniques support the validity of both. We have demonstrated that transiently negative values of both diffusion coefficients $\mathrm{ND}_{E\times B}$ and $\mathrm{ND}_E$ can be obtained by switching on an orthogonal magnetic field of a sufficient strength that the gyro-period of the electrons is less than the mean time between collisions. Finally, it should be highlighted that although the second law of thermodynamics implies that the diffusion tensor must be positive definite (and hence the diagonal elements positive) in the steady state where mechanical equilibrium has been attained [34], there are no such limitations for the time-dependent transient states considered here.

## Acknowledgments

All the authors would like to acknowledge the support of the Australian Research Council and the Centre for Antimatter-Matter studies. Three of the authors (SD, ZR and ZLjP) were partly funded by the MNTR project 14102J.

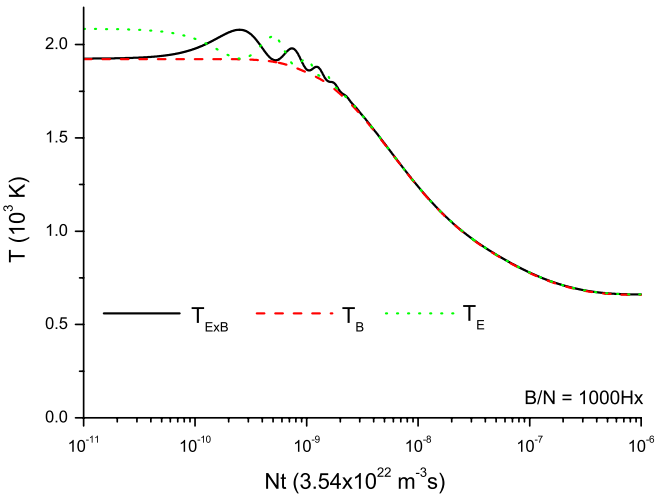


**Figure A1.** Comparison of the temporal relaxation profiles of the diagonal temperature tensor elements for various applied magnetic fields for electrons in the Reid ramp model. These results have been calculated using the time-dependent multi-term solution of Boltzmann's equation.

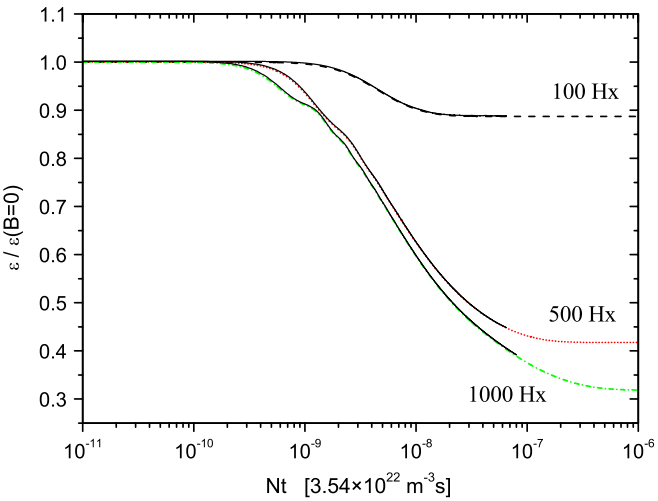


**Figure A2.** Temporal relaxation of $\varepsilon$ for various applied magnetic fields for electrons in the Reid ramp model ($E/N = 12$ Td). The dashed lines represent the results from the time-dependent multi-term solution of Boltzmann's equation while the solid lines represent those from the Monte Carlo simulation.

## Appendix A. Transient behaviour of other transport properties

Other transport properties of interest in terms of the calculated moments include:

$$\varepsilon = \frac{3}{2}kT_{\mathrm{b}}\left[1 - \sqrt{\frac{2}{3}}\Re\{F(100|000)\}\right] \quad \text{(mean energy)}, \tag{A.1}$$

$$W_E = \frac{1}{\alpha}\sqrt{2}\Im\{F(011|000)\} \quad (\boldsymbol{E}\text{-drift velocity}), \tag{A.2}$$

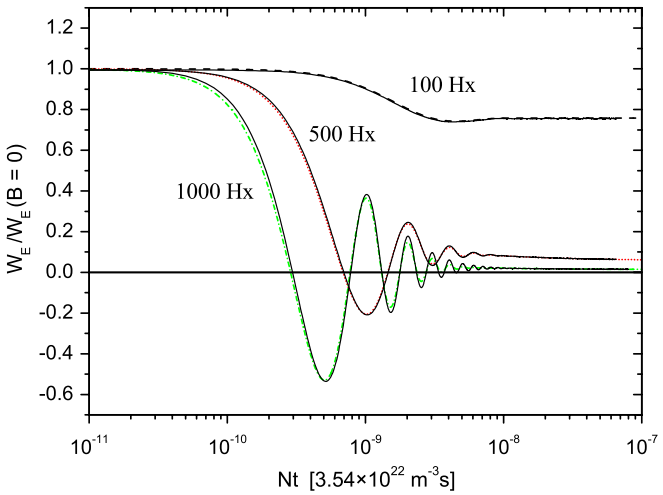


**Figure A3.** Temporal relaxation of $W_E$ for various applied magnetic fields for electrons in the Reid ramp model ($E/N = 12$ Td). The dashed lines represent the results from the time-dependent multi-term solution of Boltzmann's equation while the solid lines represent those from the Monte Carlo simulation.

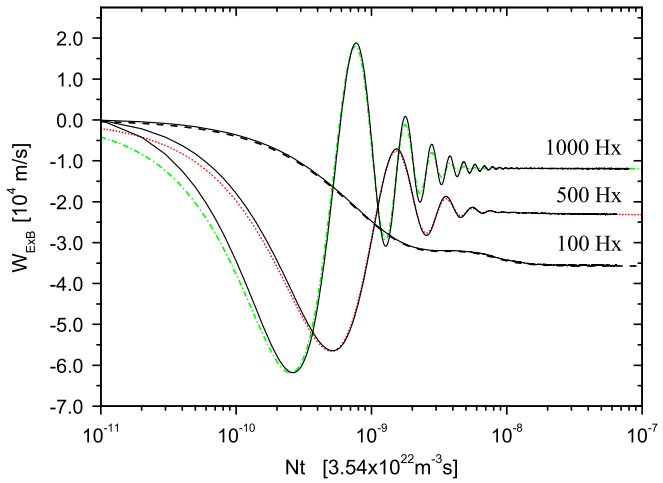


**Figure A4.** Temporal relaxation of $\varepsilon$, $W_E$ and $W_{E\times B}$ for various applied magnetic fields for electrons in the Reid ramp model ($E/N = 12$ Td). The dashed lines represent the results from the time-dependent multi-term solution of Boltzmann's equation while the solid lines represent those from the Monte Carlo simulation.

$$W_{E\times B} = -\frac{1}{\alpha}\Im\{F(010|000)\} \quad (\boldsymbol{E}\times\boldsymbol{B} - \text{drift velocity}), \tag{A.3}$$

where $\Re\{\}$ and $\Im\{\}$ refer to the real and imaginary parts, respectively. The temporal relaxation profiles for these transport properties are displayed in figures A1–A4. The transient phenomena is consistent with the behaviour demonstrated in [20]. The steady-state behaviour in $\boldsymbol{E}\times\boldsymbol{B}$ fields is in general well known [3, 25, 35–37].

## References


[1] Raspopović Z, Sakadžić S, Petrović Z Lj and Makabe T 2000 *J. Phys. D: Appl. Phys.* **33** 1298–302

[2] Petrović Z Lj, Raspopović Z M, Dujko S and Makabe T 2002 *Appl. Surf. Sci.* **192** 1–21

[3] White R D, Ness K F and Robson R E 2002 *Appl. Surf. Sci.* **192** 26–49

[4] Winkler R, Loffhagen D and Sigeneger F 2002 *Appl. Surf. Sci.* **192** 50–71

[5] Trunec D, Bonaventura Z and Necas D 2006 *J. Phys. D: Appl. Phys.* **39** 2544–52

[6] Lieberman M A and Lichtenberg A J 2005 *Principles of Plasma Discharges and Materials Processing* 2nd edn (New York: Wiley)

[7] Makabe T and Petrović Z Lj 2006 *Plasma Electronics* (Boca Raton FL: CRC/Taylor and Francis)

[8] Robson R E, White R D and Petrović Z Lj 2005 *Rev. Mod. Phys.* **77** 1303–20

[9] Maeda K and Makabe T 1994 *Phys. Scr.* T **53** 61

[10] White R D, Robson R E and Ness K F 1995 *Aust. J. Phys.* **48** 925

[11] Maeda K, Makabe T, Nakano N, Bzenić S and Petrović Z Lj 1997 *Phys. Rev.* E **55** 5901

[12] White R D, Robson R E and Ness K F 1998 *J. Vac. Sci. Technol.* E **16** 316

[13] Dujko S, Raspopović Z M and Petrović Z Lj 2005 *J. Phys. D: Appl. Phys.* **38** 2952

[14] White R D 2001 *Phys. Rev.* E **64** 056409

[15] Shizgal B and MacMahon D R A 1985 *Phys. Rev.* A **32** 3669

[16] Loffhagen D and Winkler R 1996 *J. Phys. D: Appl. Phys.* **29** 618

[17] Dyatko N A, Napartovich A P, Sakadžić S, Petrović Z Lj and Raspopović Z 2000 *J. Phys. D: Appl. Phys.* **33** 375–80

[18] Loffhagen D, Braglia G L and Winkler R 1998 *Contrib. Plasma Phys.* **38** 527

[19] Bzenić S, Raspopović Z M, Sakadžić S and Petrović Z Lj 1999 *IEEE. Trans. Plasma Sci.* **27** 78

[20] Loffhagen D and Winkler R 1999 *IEEE Trans. Plasma Sci.* **27** 1262

[21] Nakano N, Petrović Z Lj and Makabe T 1994 *Phys. Rev.* E **49** 4455

[22] Boltzmann L 1872 *Wein. Ber.* **66** 275

[23] Wang-Chang C S, Uhlenbeck G E and De Boer J 1964 *Studies in Statistical Mechanics* ed J De Boer and G E Uhlenbeck vol II (New York: Wiley) p 241

[24] Robson R E and Ness K F 1986 *Phys. Rev.* A **33** 2068

[25] Ness K F 1994 *J. Phys. D: Appl. Phys.* **27** 1848

[26] White R D, Ness K F, Robson R E and Li B 1999 *Phys. Rev.* E **60** 2231

[27] Kumar K, Skullerud H R and Robson R E 1980 *Aust. J. Phys.* **33** 343

[28] Fano U and Racah G 1959 *Irreducible Tensorial Sets* (New York: Academic)

[29] Raspopović Z M, Dujko S and Petrović Z Lj 2003 *Proc. 17th European Conf. on Atomic and Molecular Physics of Ionized Gases (Contanta, Romania)* p 47

[30] Birdsall C K and Langdon A B 1985 *Plasma Physics via Computer Simulation* (New York: McGraw-Hill)

[31] Reid I D 1979 *Aust. J. Phys.* **32** 231

[32] White R D, Brennan M J and Ness K F 1997 *J. Phys. D: Appl. Phys.* **30** 810–16

[33] Allis W P 1959 *The Encyclopedia of Physics* ed S Flugge vol XXI (Berlin: Springer) P 383

[34] deGroot S R and Mazur P 1968 *Non-Equilibrium Thermodynamics* (North-Holland: Amsterdam)

[35] Sugawara H, Yahata T, Oda A and Sakai Y 2000 *J. Phys. D: Appl. Phys.* **33** 1191

[36] Raspopović Z M, Sakadžić S, Bzenić S A and Petrović Z Lj 1999 *IEEE Plasma Sci.* **27** 1241

[37] Li B, White R D, Robson R E and Ness K F 2001 *Ann. Phys.* **292** 179–98